12th International Congress on the Deterioration and Conservation of Stone
Columbia University, New York, 2012

FABRIC INFLUENCES ON MICROCRACK DEGRADATION OF MARBLES

Victoria Shushakova,[1] Edwin R. Fuller, Jr.,[1] Florian Heidelbach[2] and Siegfried Siegesmund[1]

[1] *Geowissenschaftliches Zentrum der Universität Göttingen Goldschmidtstrasse 3, 37077 Göttingen, Germany*
[2] *Bayerisches Geoinstitut, Universität Bayreuth, Beyreuth, Germany*

Abstract

Microstructure-based finite element simulations were used to study an actual degradation phenomenon of marble structures, namely, microcracking. Microcrack nucleation and growth were characterized, as were their dependence on grain shape preferred orientation (SPO), lattice preferred orientation (LPO), grain size, marble composition and grain-boundary fracture toughness. Three extremes of shape fabric or SPOs were analyzed: equiaxed grains; elongated grains; and a mixture of equiaxed and elongated grains. Six LPOs were considered: a random orientation distribution function (ODF); an ODF with strong directional crystal texture generated via March Dollase fiber-texture; and four actual marble textures, as measured by electron-backscattered diffraction (EBSD). Three grain sizes were considered: fine grains of order 200 μm; medium size grains of order 1 mm; and large grains of order 2 mm. The fracture surface energy for the grain boundaries was chosen to be 20 % and 40 % of the fracture surface energy of a grain, so that both intergranular and transgranular fracture were possible. Simulations were performed for both heating and cooling by 50 °C in steps of 1 °C. Microcracking results were correlated with the thermoelastic responses (indicators) related to degradation. Certain combinations of SPO, LPO, grain size, grain-boundary fracture toughness and marble composition were shown to have a significant influence on the thermal-elastic response of marble. For instance, thermal stresses and elastic strain energy were a strong function of LPO. With increasing LPO the strain energy density and the maximum principal stress decreased. Given the same morphological properties and crystallographic texture, calcite showed larger thermal stresses than dolomite, as well as calcite has an earlier onset of microcracking upon heating and cooling, and a greater area of microcracking at a given temperature differential.

Keywords: marble, finite element simulations, EBSD, microcracking, elastic strain energy density, maximum principal stress, thermal expansion anisotropy

1. Introduction

Marble has been used as decorative and construction material for centuries. Many historical monuments, sculptures, and façade claddings are made from marble due to its workability, pureness and bright colour. However, marbles can be particularly sensitive to weathering and to degradation, and hence can have limited durability. Such deterioration phenomena depend mainly on ambient climate. Many experimental studies have shown that heating and cooling are responsible for the degradation of marble, e.g., (Kessler 1919), (Battaglia et al. 1993), (Winkler 1994), (Siegesmund et al. 2000),

(Zeisig et al. 2002). Studies of the mechanisms of deterioration are important for protecting historical heritage.

The main rock forming minerals in marble, calcite and dolomite, have large anisotropy in their coefficients of thermal expansion. Due to the thermal expansion anisotropy between the adjacent crystalline grains residual stresses are generated predominately at triple junctions and along the grain boundaries, which governs a granular decohesion of stone with time (Siegesmund et al. 2000).

Microstructure-based finite element analysis was used to elucidate these stresses and to simulate an actual degradation phenomenon, microcracking. Such modelling is in good agreement with actual experiments. It has been showed in experimental studies by (Ruedrich et al. 2002), (Zeisig et al. 2002) and (Siegesmund et al. 2008) that the shape preferred orientation (SPO), lattice preferred orientation (LPO), and grain size can cause different amounts of residual strain. (Shushakova et al. 2010) pointed out that certain combinations of SPO, LPO, and their directional relationship have significant influence on the thermomechanical response of marbles.

The goal of the present study is to investigate crack initiation and propagation, as well their dependence on different fabric parameters. Simulations were performed for both heating and cooling by 50 °C in steps of 1 °C. Microcracking results were correlated with the thermoelastic responses related to degradation, such as elastic strain energy density and maximum principal stress.

2. Methods

2.1 Shape fabric and textures

Microstructure is the geometric input for simulations via finite element analysis. To investigate the influence of shape fabric on thermoelastic response, several extremes of SPOs were analyzed: equiaxed grains; elongated grains; and a mixture of equiaxed and elongated grains (Figure 1). Microstructures were generated by a grain growth algorithm, details could be found in (Ito and Fuller 1993); (Saylor et al. 2004); (Saylor et al. 2007), (Shushakova et al. 2010). The microstructural images have a resolution of 1,000 x 1,000 pixels.

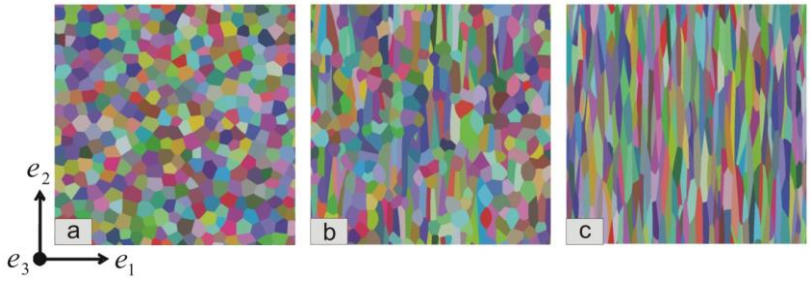

Figure 1. Microstructures used for the finite element analysis: **a.** an equiaxed microstructure of 382 grains; **b.** a mixed microstructure of 347 grains; **c.** an elongated microstructure of 312 grains. The coordinate system, $\boldsymbol{e_i}$, is also indicated, where the $\boldsymbol{e_2}$ direction is parallel to the SPO; the $\boldsymbol{e_1}$ direction is perpendicular to the SPO and in the plane of the microstructure; and the $\boldsymbol{e_3}$ direction is perpendicular to the SPO and out of the plane of the microstructure.

Orientations assigned to each grain were either generated from a March-Dollase fiber texture orientation distribution functions (ODF), (Dollase 1986) and (Blendell et al. 2004), (see Figure 2), or measured with electron back-scattered diffraction (EBSD) on actual marble samples (see Figure 3).

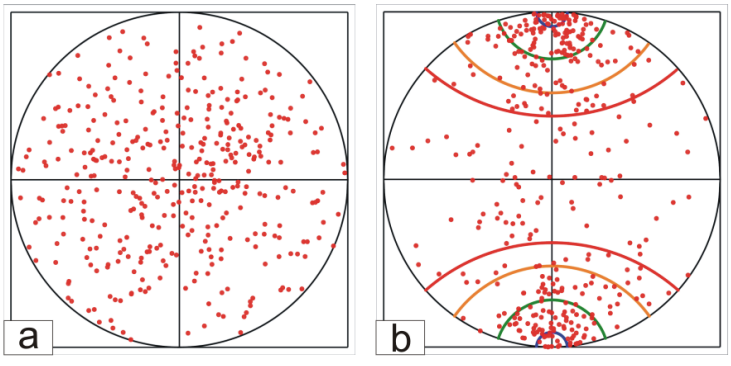

Figure. 2. Representative pole figures showing individual poles of the crystallographic c-axis for each grain in the microstructure. **a.** The orientations chosen from a random ODF (denoted M=1). **b.** The orientations chosen from a March-Dollase ODF with fiber texture that is 20 times random along the North and South pole (denoted M=20). The contour lines correspond to multiple random distribution (MRD) from the March-Dollase distribution function of 16 (blue: nearest to NS pole), 4 (green), 1 (orange), and 1/2 (red: nearest to the equator).

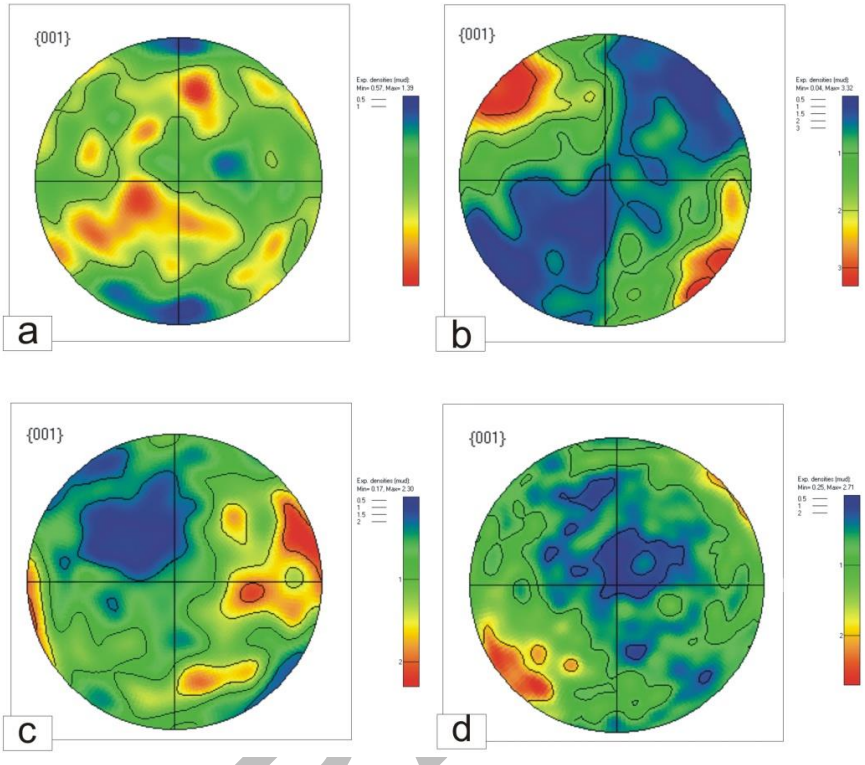

Figure 3. {001} Pole figures from the EBSD HKL Channel 5 software for marble samples in xz planes: **a.** Arabescaro Altissimo (Carrara marble from Italy); **b.** Sölk (calcitic marble from Austria); **c.** Lasa (calcitic marble from Italy); **d.** HT-Carrara (Carrara marble from Italy).

Six different LPOs were considered: a random ODF; an ODF with strong directional crystal texture generated via March-Dollase fiber-texture with a maximum multiple random distribution (MRD) of 20; and four actual marble textures, as measured with EBSD with maximum MRDs from 1 (Arabescaro Altissimo) to 3 (Sölk). The algorithm implemented to generate the March-Dollase ODFs is described elsewhere (Saylor et al. 2007; Shushakova et al. 2010). The c-axis crystal texture was parallel to the $\boldsymbol{e_3}$ direction (see Figure 1).

ODFs were measured with EBSD for four marble types: a Carrara marble with weak LPO; a Sölk marble with more pronounced LPO; a Lasa marble with a c-axis girdle distribution; and a HT-Carrara with high temperature texture. The orientations of the individual grains in the microstructure were determined by EBSD. Only a small fraction of the orientations were randomly assigned to the idealized microstructures, i.e., 382 grain orientations for the equiaxed microstructure, 347 orientations for the mixed microstructure and 312 for the elongated microstructure.

2.2 Finite-element simulations

The microstructure-based finite-element approach used here is based on the Object-Oriented Finite Element program OOF developed at the National Institute of Standards

and Technology (Langer et al. 2001). The OOF software is in the public domain. Executables, source code, and manuals are available at:
http://www.nist.gov/mml/ctcms/oof/. The OOF1 software was used here.

An adaptive meshing algorithm was implemented to create a mesh with a grain-boundary phase that has the same thermo-elastic properties as the grains, but with a different fracture toughness. The final mesh consisted of 140,358 elements for the equiaxed microstructure, 207,208 elements for the mixed microstructure and 163,668 elements for the elongated microstructure. After the mesh was generated, thermal and elastic properties of calcite and dolomite (Table 1) were assigned to the constituent grains.

Table 1. The single-crystal elastic constants, $\boldsymbol{C_{ij}}$, in GPa (Bass 1995) and the crystalline coefficients of thermal expansion, $\boldsymbol{\alpha_{ij}}$, in 10^{-6} °C^{-1} for calcite (Kleber 1959) and dolomite (Reeder and Markgraf 1986).

Material	C_{11}	C_{12}	C_{13}	C_{14}	C_{15}	C_{33}	C_{44}	α_{11}	α_{33}
Calcite	144.0	53.9	51.1	-20.5	0	84.0	33.5	-6.0	26.0
Dolomite	205	70	57.4	-19.5	13.7	113.0	39.8	6.0	26.0

In the microcracking simulations three grain sizes were considered: fine grains of order 200 µm (calcitic marble); medium size grains of order 1 mm (calcitic and dolomitic marbles); and large grains of order 2 mm (dolomitic marble). The grain-boundary fracture surface energy, γ_{ig}, was chosen to be 20 % and 40 % of the crystalline fracture surface energy, γ_{xtal}, so that both intergranular and transgranular fracture were possible. The crystalline, or grain fracture toughness, γ_{xtal}, was assumed to be 0.5 Jm^{-2} and isotropic. For these configurations the following fabric parameters were used: equiaxed; mixed; and elongated microstructures with random texture and strong texture generated via a March-Dollase distribution. Three replications of orientations were generated for calcite microstructures with a grain size of 1 mm and a grain boundary toughness of 0.40 γ_{xtal}. For the other combinations of fabric parameters only one set of orientations was generated to elucidate fabric effects. Textures from four actual calcitic marble types were used in simulations with both equiaxed and elongated microstructures with a grain size of 1 mm and a grain boundary toughness of 0.40 γ_{xtal}. Hereby, 50 unique configurations were used as the basis for the finite-element simulations.

The finite-element calculations are based on two-dimensional plane-stress elasticity, and thereby simulated the results for a free surface. The typical thermoelastic responses that are computed are the maximum principal stress and the elastic strain energy density. A microcracking algorithm, as described in (Zimmermann et al. 2001) and (Galal Yousef et al. 2005), was used to initiate and propagate microcracks.

3. Results

3.1 LPOs generated via March Dollase distribution

The elastic strain energy density can be considered as a key precursor of potential microcracking in a microstructure. It provides the surface energy necessary to create the fracture surfaces of the microstructural cracks. To elucidate factors related to marble degradation due to microcracking phenomena, the influence of SPO, LPO, grain size,

grain boundary toughness and marble composition on the elastic strain energy density were studied by microstructural simulations.

The elastic strain energy density was monitored during heating and cooling for temperature step changes of 1 °C for both cracked and uncracked samples. The uncracked simulations are those for which no microcracking was allowed. The thermoelastic response values are plotted for the temperature interval from 10 °C to 50 °C during heating and from −10 °C to −50 °C during cooling (see Figure 4). Since elastic strain energy is converted to fracture surface energy on microcracking, one suspects that in the equiaxed microstructure one would have more microcracking with random crystallographic texture than with strong fiber texture (M=20). To verify this conjecture, the percentage of microcracked elements versus the heating or cooling temperature change is displayed in Figure 5, where this is demonstrated.

More microcracking is observed in the equiaxed microstructure with random texture upon heating (7.6 % of the total area at $\Delta T = 50$ °C) and cooling (9.5 % at $\Delta T = -50$ °C) than in the mixed grain-size microstructure with random texture, where only 5.6 % of whole area is cracked upon heating and 7.6 % upon cooling. Even fewer elements are cracked in the elongated microstructure with random texture: 4.4 % and 8.3 % upon heating and cooling, respectively. In all microstructures more microcracking is observed upon cooling, than upon heating, which results from the asymmetry in the thermal expansion along the c- and a-axes with respect to the average thermal expansion. A basic observation is that the strain energy density and the percentage of microcracked elements due to heating and cooling depend significantly on both SPO and LPO. When texture is twenty times random less microcracking is observed in the elongated microstructure upon heating (0.2 % of the total area at $\Delta T = 50$ °C) and cooling (2.7% at $\Delta T = -50$ °C) in comparison with the equiaxed microstructure where 3.9 % of whole area is cracked upon heating and upon cooling, and with the mixed microstructure where 2.1% and 3.3% is observed, respectively.

To investigate the relation between maximum principal stress and microcracking initiation, high-stress regions in an uncracked material were compared to the microcracks in the cracked material. Microstructural maps show the spatial dependence of maximum principal stress for the equiaxed microstructure with the random texture (see Figure 6), when $\Delta T = 50$ °C and $\Delta T = -50$ °C in uncracked and cracked materials. The regions with high maximum principal stress in the uncracked state correspond to microcracks in the cracked material.

It is evident that microcracks that occurred upon heating do not form upon cooling and vice versa (Weiss et al. 2002).

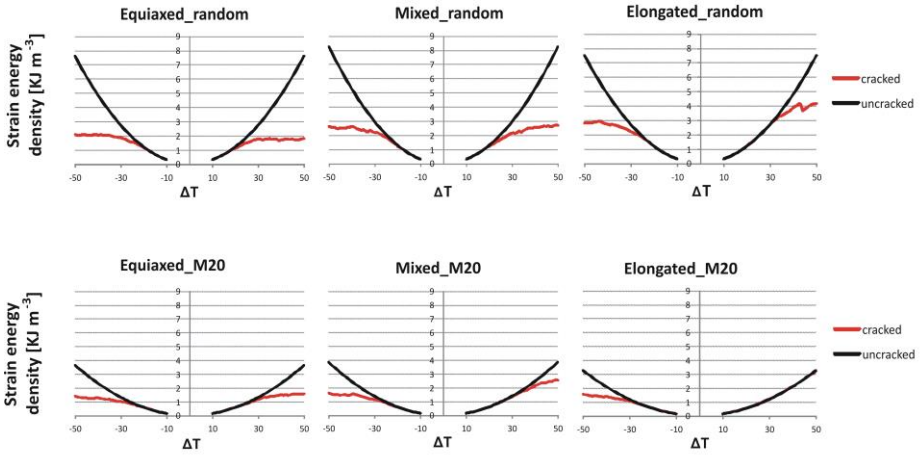

Figure 4. Elastic strain energy density for microcracked and unmicrocracked idealized marble microstructures versus the temperature change from the unstressed state. Results are shown for three idealized calcitic microstructures (equiaxed grains; mixture of equiaxed and elongated grains; and elongated grains) and for two LPOs: random texture and 20 times random texture (denoted as M20) with a grain size of 1 mm and a grain boundary toughness 0.40 γ_{xtal}.

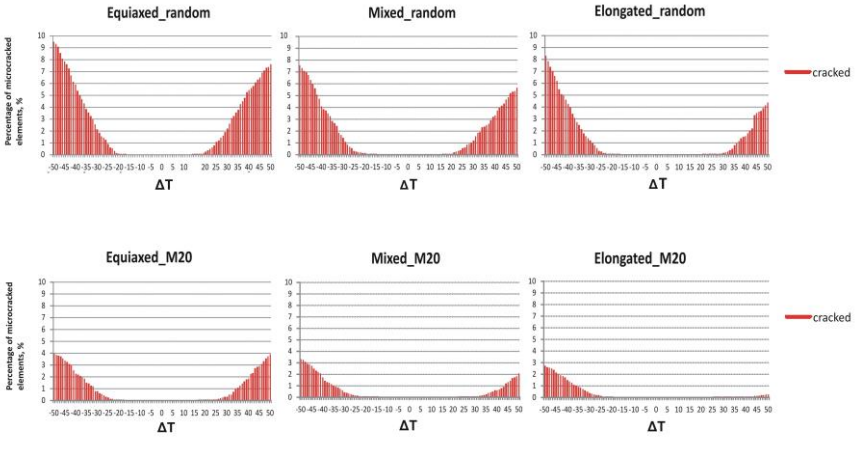

Figure 5. Percentage of microcracked elements for the three idealized marble microstructures with two textures: random texture and 20 times random texture (denoted as M20).

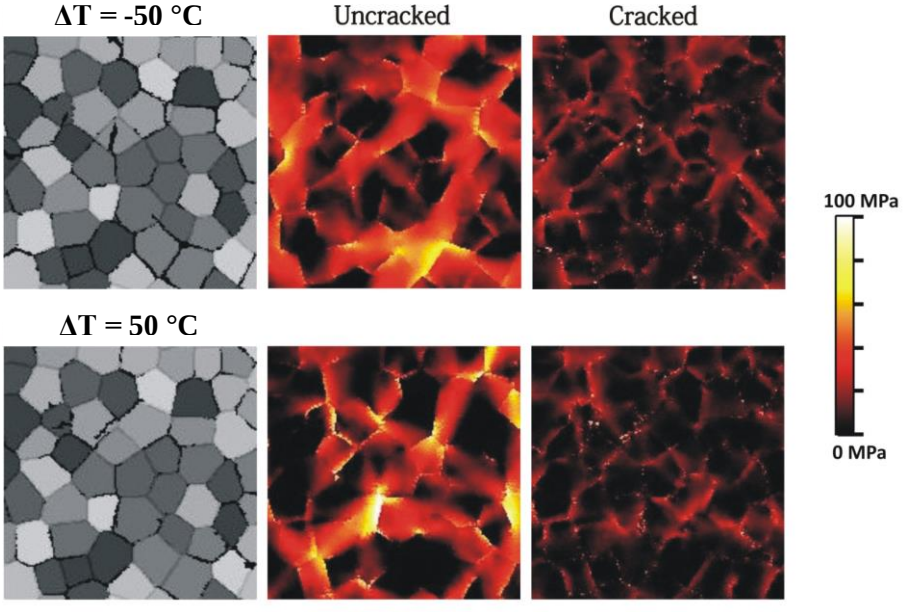

Figure 6. Representative microstructural maps showing the spatial dependence of the maximum principal stress for an equiaxed calcitic marble microstructure with a random ODF, grain size of 1 mm, and grain boundary toughness of 0.40 γ_{xtal}, when ΔT=−50 °C and ΔT=50 °C in uncracked and cracked materials. Black regions in the micrographs show the microcracks. Stresses in the maps are shown with a *thermal* scale that ranges from black (0 MPa) to white (≥ 100 MPa).

To investigate effect of grain boundary toughness on the resultant microcracking, simulations were performed for a dolomitic marble with a grain size of 1 mm. More microcracking was observed for the case of a grain boundary toughness of 0.20 γ_{xtal} than for 0.40 γ_{xtal}. Moreover, simulations with a grain boundary toughness of 0.20 γ_{xtal} commences to microcrack at a lower temperature differential. Results are shown in Figure 7. When grain boundary toughness is 20 % of γ_{xtal}, intragranular cracking is reduced or vanishes completely.

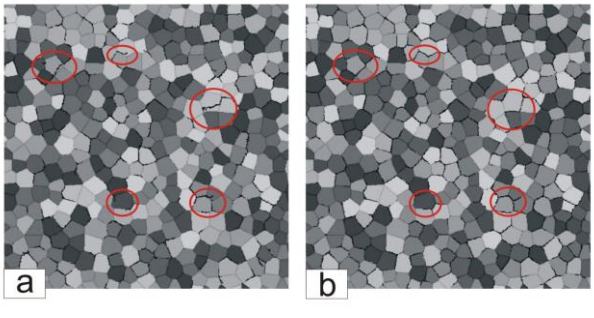

Figure 7. Simulations of microcracking in a dolomite marble with a grain size of 1 mm upon heating by a temperature differential of 50 ˚C: **a.** equiaxed microstructure with random texture and

grain boundary toughness of 0.40 γ_{xtal}; **b.** equiaxed microstructure with random texture and grain boundary toughness of 0.20 γ_{xtal}.

To elucidate the influence of grain size and marble composition, calcitic microstructures with grain sizes of 200 μm and 1 mm, and dolomitic microstructures with grain sizes of 1 mm and 2 mm were analyzed. With increasing grain size for both calcitic and dolomitic marbles, the percentage of microcracked elements is greater and microcracks occur at a lower temperature differential. For instance, an equiaxed microstructure with a grain size of 200 μm and calcitic thermo-elastic properties has only 0.5 % of microcracked area at $\Delta T = 50$ °C and microcracking commences at 31 ˚C, while the same calcitic microstructure with a grain size of 1 mm has 7.6 % of microcracked area at $\Delta T = 50$ °C and starts to crack at 14 ˚C. For dolomitic microstructures the increase of microcracked area is not extremely large: it is approximately two times larger for the case of the grain size of 2 mm compared to 1 mm (i.e., 4.9 % of .microcracked area at $\Delta T = 50$ °C in the equiaxed microstructure with the grain size 1 mm in comparison with 8.4 % at $\Delta T = 50$ °C of microcracked area in the microstructure with the grain size 2 mm).

The comparison of the results for microstructures with a grain size of 1 mm but different marble composition revealed that the dolomitic marble has less of a tendency for microcracking, i.e., microcracking begins at a higher temperature differential, and the percentage of cracked area is reduced by 1.5 times in comparison with a calcitic marble. While dolomite is stiffer than calcite, calcite has a greater thermal expansion anisotropy, resulting in a higher maximum principal stress. The percentage of microcracked area in the dolomitic marble with a grain size of 2 mm is comparable with results for the calcitic marble with a grain size of 1 mm.

3.2 LPO measured on four actual marbles with EBSD:

The simulations were performed for equiaxed and elongated calcitic microstructures with a grain size of 1 mm and a grain boundary toughness of 0.40 γ_{xtal}. The percentage of microcracked area (Table 2) for an equiaxed microstructure with the random texture (Arabescaro Altissimo marble), girdle texture (Lasa marble) and high-temperature texture (Carrara marble) upon heating and cooling is comparable with the results of simulations for microstructure with equiaxed grains with random texture generated via March Dollase distribution. For stronger texture (Sölk marble) this value is smaller, but not significantly. Elongated microstructures with the girdle texture exhibited by Lasa marbles show the smallest percentage of microcracked elements. This type of texture has *not* been simulated for idealized ODFs. Elongated microstructures with random texture (i.e., Arabescaro Altissimo) and with more pronounced LPO (i.e., Sölk) have similar amounts of microcracking.

Table 2. The percentage of the microcracked area for equiaxed and elongated microstructures at $\Delta T = 50$ °C upon heating and at $\Delta T = -50$ °C upon cooling.

Marble sample	Percentage of microcracked elements			
	Heating		Cooling	
	Equiaxed	Elongated	Equiaxed	Elongated
Arabescaro Altissimo	7.6%	4.2%	8.4%	5.3%
Sölk	7.1%	4.4%	7.6%	5.4%

Lasa	7.6%	1.5%	8.7%	2.6%
HT-Carrara	8.0%	5.2%	9.1%	5.8%

The influence of SPO is significant. For microstructures with elongated grains the percentage of microcracked elements is reduced by 1.5 times. Similar to the results for the idealized LPOs, there is less microcracking upon heating than upon cooling.

4. Discussion and Conclusions

Many fabric parameters influence thermal degradation of marbles. Most of them have been investigated in the present study. It was shown that lattice preferred orientation (LPO), shape preferred orientation (SPO), grain size, grain boundary toughness and marble composition control the thermoelastic response of marble microstructures. The present investigation revealed that with decreasing grain size and increasing LPO and SPO microcracking is less and it commences at greater temperature differentials. It was observed that microcracking upon heating is generally less than upon cooling. Dolomitic marbles have less of a tendency to microcrack. While dolomite is stiffer than calcite, calcite has a greater thermal expansion anisotropy, thus resulting in higher maximum principal stresses. In agreement (Zeisig et al. 2002) experimentally showed that dolomitic marbles do not have residual strains after thermal treatment.

Microstructural maps were generated that show the spatial dependence of the maximum principal stress. To investigate the relation between maximum principal stress and microcracking initiation, high-stress regions in an uncracked material were compared to the microcracks in the cracked material. The regions with high maximum principal stress in uncracked state correspond to microcracks in the cracked material.

Simulations that used textures from actual marble samples showed results that are comparable with results from simulations with the March-Dollase generated ODFs.

In summary, microstructure-based finite-element simulations are an excellent tool for elucidating influences of the rock fabric and crystal texture on the thermoelastic behavior and microcracking response of marbles.

Acknowledgments

Financial support for E. R. Fuller, Jr. at Universität Göttingen was provided by the Deutsche Forschungsgemeinschaft grant: SI 438/39-1, and is gratefully acknowledged. Victoria Shushakova gratefully acknowledges a long-term DAAD fellowship grant.

References

Bass, J.D. 1995. 'Elasticity of minerals, glasses, and melts', *Handbook of Physical Constants*, (ed. Ahrens, T.J.) 45-63. Washington, D.C.: American Geophysical Union.

Battaglia, S., Franzini, M., Mango, F.. 1993. 'High sensitivity apparatus for measuring linear thermal expansion: preliminary results on the response of marbles', *II Nuovo Cimento,* **16:** 453-461.

Blendell, J.E., Vaudin, M.D., Fuller, E.R., 2004. 'Determination of texture from individual grain orientation measurements', Journal of the American Ceramic Society, **82**(11): 3217-3220.

Dollase, W.A., 1986. *Journal of Applied Crystallography*, **19**:267-272.

Galal Yousef, S., Rödel, J., Fuller, E.R., Zimmermann, A, El-Dasher, B.S., 2005. 'Microcrack Evolution in Alumina Ceramics: Experiment and Simulation', *Journal of the American Ceramic Society*, **88**(10): 2809-2816.

Ito, O., Fuller, E.R., 1993. 'Computer modelling of anisotropic grain microstructure in two dimensions', *Acta Metallurgica et Materialia*, **41**(1):191-198.

Kessler, D.W., 1919. 'Physical and chemical tests on the commercial marbles of the United States', Technologic Papers Bureau of Standards, No. 123. Washington, D.C., Government Printing Office.

Kleber, W., 1959. *Einfiihrung in die Kristallographie*, Berlin: Verlag Technik, Berlin.

Langer, S.A., Fuller, E.R., Carter, W.C., 2001. '*Computing in Science and Engineering*', **3**:15-23.

Reeder, R., Markgraf, S.A., 1986. 'High temperature crystal chemistry of dolomite,' *American Mineralogist*, **71**:795-804.

Ruedrich, J., Weiss, T., Siegesmund, S., 2002. 'Thermal behaviour of weathered and consolidated marbles', *Natural Stone, Weathering Phenomena, Conservation Strategies and Case Studies*, (eds Siegesmund, S., Weiss, T., Vollbrecht, A.), Geological Society, London, **205**:255-271.

Saylor, D.M., Fridy J., El-Dasher B.S., Jung K.Y., Rollett, A.D., 2004. 'Statistically representative three-dimensional microstructures based on orthogonal observation sections', *Metallurgical and Materials Transactions A*, **35A**:1969-1979.

Saylor, D.M., Fuller, E.R., Weiss, T., 2007. 'Thermal-elastic response of marble polycrystals: Influence of grain orientation configuration', *International Journal of Materials Research*, (formerly Z. Metallkd.) **98**(12):1256-1263.

Shushakova, V., Fuller, E.R., Siegesmund, S., 2010. 'Influence of shape fabric and crystal texture on marble degradation phenomena: simulations', *Environmental Earth Sciences*, doi: 10.1007/s12665-010-0744-7.

Siegesmund, S., Ullemeyer, K., Weiss, T., Tschegg, E.K., 2000. 'Physical weathering of marbles caused by anisotropic thermal expansion', *International Journal of Earth Science*, **89**:170-182.

Siegesmund, S., Ruedrich, J., Koch, A., 2008. 'Marble Bowing: Comparative studies of different public building facades', *Environmental Geology*, **56**:473-494. In *Monumental future: climate change, air pollution, stone decay and conservation*, (eds Siegesmund, S., Snethlage. R., Ruedrich, J.)

Weiss, T., Siegesmund, S., Fuller, E.R. 2002. 'Thermal stresses and microcracking in calcite and dolomite marbles via finite element modelling', *Natural Stone, Weathering Phenomena, Conservation Strategies and Case Studies*, (eds Siegesmund, S., Weiss, T., Vollbrecht, A.), Geological Society, London, **205**:89-102.

Winkler, E.M. 1994. *Stone in Architecture: Properties, Durability*. Berlin: Springer-Verlag.

Zeisig, A., Siegesmund, S., Weiss, T.., 2002. 'Thermal expansion and its control on the durability of marbles', *Natural Stone, Weathering Phenomena, Conservation Strategies and Case Studies*, (eds Siegesmund, S., Weiss, T., Vollbrecht, A.), Geological Society, London, **205**:65-80.

Zimmermann, A., Carter, W.C., Fuller, E.R. 2001. 'Damage Evolution During Microcracking of Brittle Solids', *Acta Materialia*, **49**:127-137.